Wireless link evaluation of a dielectric resonator nanoantenna

Gilliard N. Malheiros-Silveira*[a,b], Ruth E. Rubio-Noriega[c], and Hugo E. Hernandez-Figueroa[b]
[a]São Paulo State University (UNESP), Campus of São João da Boa Vista, São Paulo, Brazil.
[b]School of Electrical and Computer Engineering (FEEC), University of Campinas (UNICAMP), São Paulo, Brazil.
[c]Instituto Nacional de Investigación y Capacitación de Telecomunicaciones (INICTEL) - Universidad Nacional de Ingeniería (UNI), Lima, Peru.
*gnmsilveira@gmail.com

ABSTRACT

Optical antennas/nanoantennas are optical elements that have gained highlight in this decade and have potential application in several branches of photonics/plasmonics, such as, optical sensors, lasers, solid state lighting, photovoltaics, microscopy, etc. Additionally, the dipole nanoantennas have been the antennas elements mostly studied in proposals for those applications and, in special, for free-space communication based on plasmonic circuits.

Here we report some advantages of dielectric resonator nanoantennas (DRNAs) as elements for coupling light to plasmonic-based circuits. Fundamental antenna parameters such as reflection coefficient, gain, efficiency, among others, are evaluated and its advantages are highlighted for nanophotonics applications. A study about an optical link for circuits based on metal-dielectric-metal-dielectric (MDMD) nanostrip waveguides operating at the central wavelength of λ_0 = 1.55 μm is evaluated. We studied the coupling of near- and far-fields of a DRNA matched to an MDMD nanostrip waveguide. The results show the advantage of it as an element for optical coupling from/to free-space as well as to establish a wireless optical link for inter-chip communication.

Keywords: plasmonics; nanoantennas; wireless optical link; optical antennas.

1. INTRODUCTION

The advent of metallic components with high modal optical confinement used for electric field enhancement or for light propagation has encouraged the development of several applications based on plasmonic components and circuits [1]–[6]. Plasmonic components when compared to dielectric ones [7], [8] are ultra-compact however they suffer for metal absorption losses, thus limiting realization of integrated circuits with relatively long propagation distances. The proposal of a wireless link to reduce the propagation losses between two distant points was already proposed assuming dipole nanoantennas integrated to plasmonic waveguides operating at f_0 = 415 THz [9]. In this manuscript, a theoretical study about optical coupling for circuits based on nanostrip waveguides [10] operating at the central wavelength of λ_0 = 1.55 μm is evaluated. We investigate the potential of a nanoscale version of a dielectric resonator antenna [11], i.e., DRNAs [12]–[18] as an approach to facilitate the implementation of wireless optical links based on plasmonic nanostrip waveguides.

2. MATERIALS, METHODS, AND RESULTS

Figure 1(a) shows a schematic of a DRNA coupled to a nanostrip waveguide. Fig. 1 (b)-(c) show the DRNA and nanostrip dimensions for which, the optimized values assume: h_1 = 0.145 μm, h_2 = 0.020 μm, h_3 = 0.010 μm and w = 0.340 μm [12]. The metallic regions are composed of Ag [19], and the low index dielectric is composed of SiO_2.

Optical Interconnects XIX, edited by Henning Schröder, Ray T. Chen, Proc. of SPIE Vol. 10924
109241A · © 2019 SPIE · CCC code: 0277-786X/19/$18 · doi: 10.1117/12.2510605

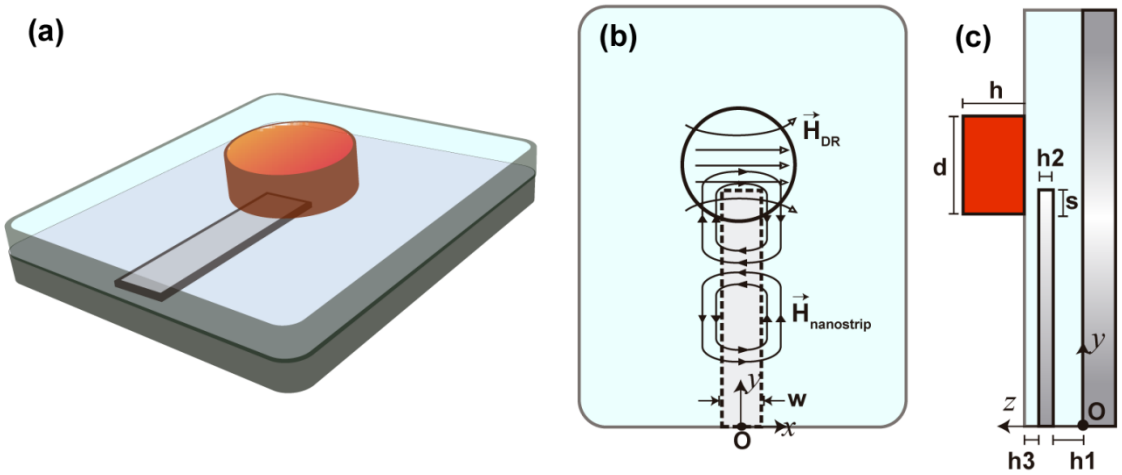

Figure. 1. (a) 3-D schematic of a DRNA integrated to a nanostrip waveguide. (b) NDRA top view: magnetic field lines showing the compatibility coupling between the fundamental nanostrip mode and the DR's $HE_{11\delta}$ mode. (c) NDRA lateral view: the layers present in the NDRA feeding geometry and their respective thickness parameters [12].

A dielectric resonator (DR) composed by a-Si with d = 0.490 μm and h = 0.315 μm is positioned in a way of matching its fundamental mode to the fundamental mode of the nanostrip waveguide.

The return loss (S_{11}) curve shown in Fig. 2(a), exhibits a resonance at 193.5THz (λ_0=1.55μm) with pronounced deep about -32 dB, and a relatively wideband for values below -10dB and -15dB, approximately 20 THz and 13.4 THz, respectively. The -10dB S_{11} band covers practically three optical communication bands: L-band (1.565-1.625μm = 0.06μm), C-band (1.530-1.565μm = 35μm), and S-band (1.460-1.530μm = 70μm). Along the -10 dB S_{11} band the radiation patterns maintain very similar shapes with a very directive main lobe and small gain variation around 7.5dB (see Figs.2 (c)(e)(g)). In our simulations, we have observed that the $HE_{11\delta}$ mode is excited between 185 THz and 196 THz, and the $HE_{12\delta}$ mode between 196 THz and 205 THz, within the -10dB S_{11} band.

This NDRA exhibits broadside radiation - as shown in Figs. 2(c)(e)(g) - i.e., the radiating power flows parallel to the z-axis.

The magnetic fields coupled from the nanostrip to the DR (as depicted in Fig.1(b)) are shown in Fig. 3(a) by the contour plots taken at planes z =g/2=0.075μm (left picture) and z = g+t+p+h/2=0.335μm (right picture). Fig. 3 (b) shows the near field's phase displacement at 193.5THz (λ_0=1.55μm), across the DR's cross-section.

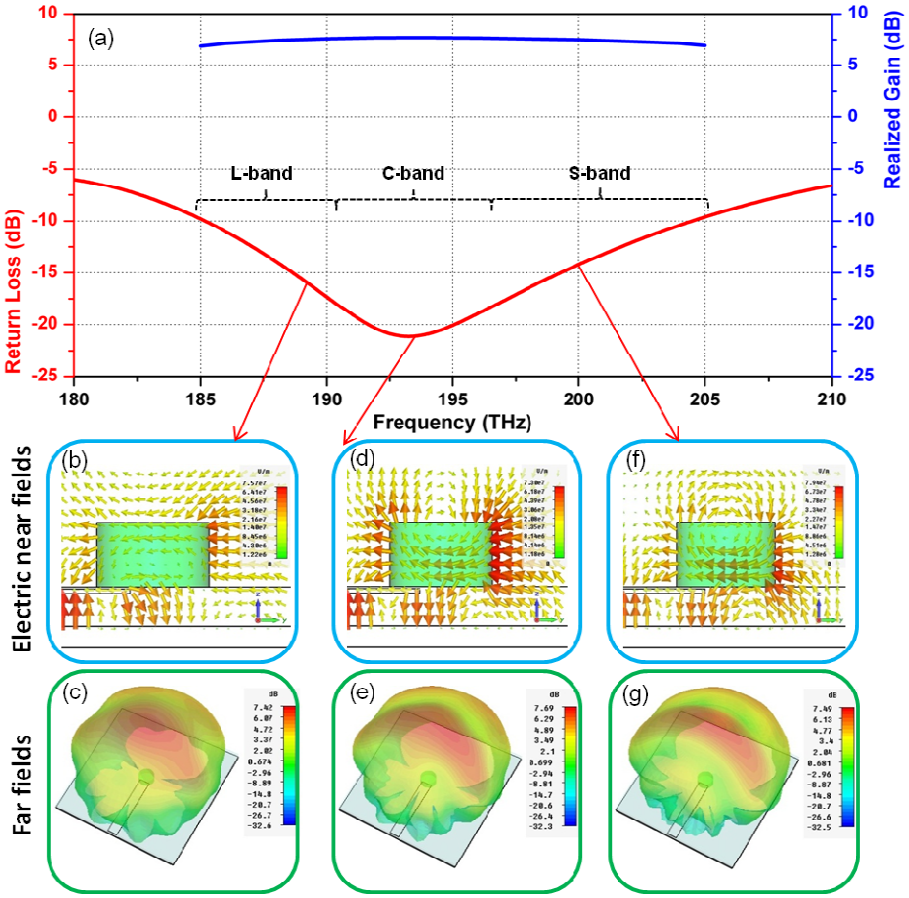

Figure 2. Fundamental parameters of the antenna depicted in Fig. 1. (a) Return loss, S_{11}, and gain curves. (b), (c) Electric near field and 3D radiation pattern at 188THz (1.60μm), respectively. (d),(e) Electric near field and 3D radiation pattern at 193.5THz (1.55μm), respectively. (f),(g) Electric near field and 3D radiation pattern at 199THz (1.50μm), respectively.

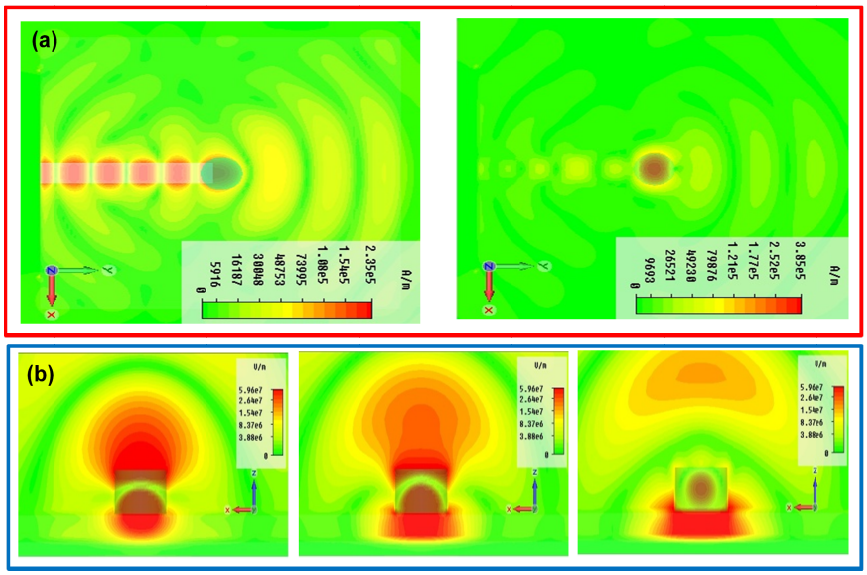

Figure 3. (a) Modulus of the magnetic fields distribution at the DRNA. (left) magnetic field between nanostrip and ground plane and (right) magnetic field at DR cross-section of the NDRA at half height. (b) Cross-sections of the DRNA showing the electric field modulus behavior at 193.5THz for relative phase variation, from left to right, of 0°, 45°, and 90°, respectively.

Fig. 4(a) shows the coupling efficiency, assuming different numerical apertures from a Gaussian beam spot, 0.5 μm distant from the DRNA. The optimal position for coupling efficiency is obtained when there is an offset of about x = -0.25 μm between the center of the DR and the center of the beam. The coupling efficiency is also evaluated for the same nanostrip without a DRNA as shown in Fig. 4(b). For this case, the beam spot is located 0.5 μm distant from the nanostrip.

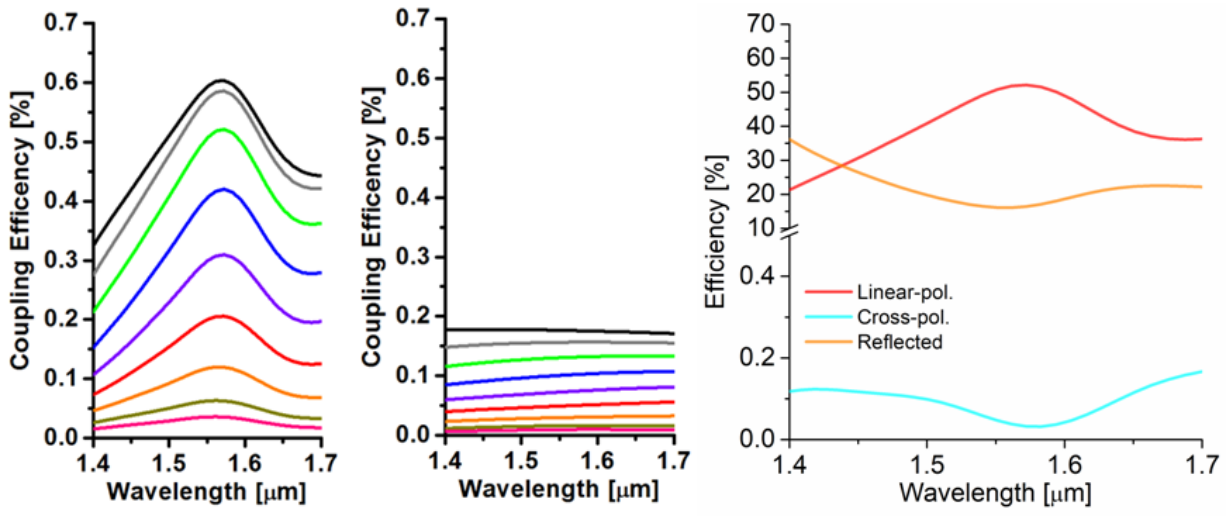

(a) (b) (c)

Figure 4. Coupling efficiency, in near field, assuming different numerical apertures from the incident field [18]: (a) Nanostrip with DR, and (b) Nanostrip without DR. (c) Comparison of the coupling efficiency, in RX mode and near field, for linear (in red) and cross-polarizations (in blue). The reflected power (in orange) through the top region is shown for the case of linear polarization.

Figure 4(c) shows the transmission and reflection of the DRNA operating in RX mode under incidence of a source of light with NA = 0.7, located 0.5 μm from the top edge of the DRNA. Coupling efficiency of about 51% is obtained at the central wavelength of 1.55 μm. At this wavelength, the reflected power through the top region is about 16% of the incident one. For this same configuration, but in cross-polarization, the coupling efficiency is below 0.1%, demonstrating right polarization sensitivity.

The power received by one antenna from another one, under idealized conditions, a distance away is given by the Friis transmission equation [20]:

$$\frac{P_r}{P_t} = \eta_t \eta_r D_t D_r \left(1-|\Gamma_t|^2\right)\left(1-|\Gamma_r|^2\right)\left|a_t . a_r^*\right|^2 \frac{\lambda_o^2}{(4\pi d)^2} \quad (1)$$

where η_t and η_r are the efficiency of the optical radiation from the transmitting and receiving antennas, respectively. D_t and D_r are the directivities of the transmitting and receiving antennas. Γ_t and Γ_r are the reflection coefficient of the link between DRNA and the plasmonic waveguide for the transmitting and receiving antennas, respectively. $a_t.a_r$* are related to the polarization matching, which can be deteriorated due to the misalignment between the two antennas. λ_0 is the wavelength of operation and d is the separation distance between the antennas. P_r is the received power at the receiving antenna and P_t is the feeding power in the transmitting antenna.

Figure 5(a) shows a schematic of a wired link based on MDMD nanostrip waveguide and a wireless link [fig. 5b] established by two DRNAs where the broadside characteristic is highlighted.

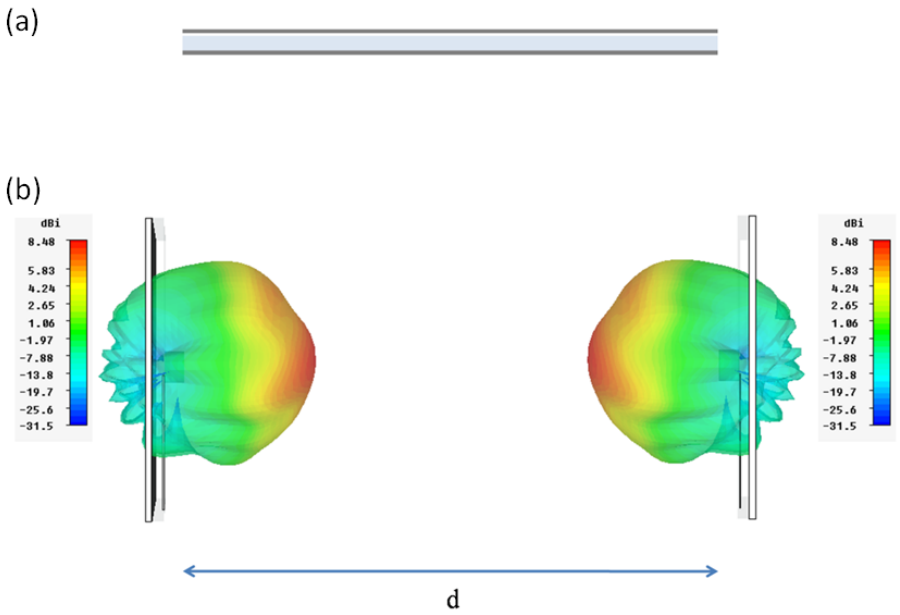

Figure 5. (a) Schematic of wired link (MDMD nanostrip waveguide) compared to a (b) wireless one. Both links assume the same separation distance, *d*.

Figure 6 shows a comparison between the interconnection of two points distant away connected by an MDMD nanostrip waveguide (wired link) and a wireless link by means of DRNAs [18] as depicted in Fig. 5a and Fig. 5b, respectively. For the wired link, the propagation is proportional to $e^{-\alpha d}$, it can be noticed that for distances longer than $d \sim$ 42 μm, the wireless link becomes more efficient.

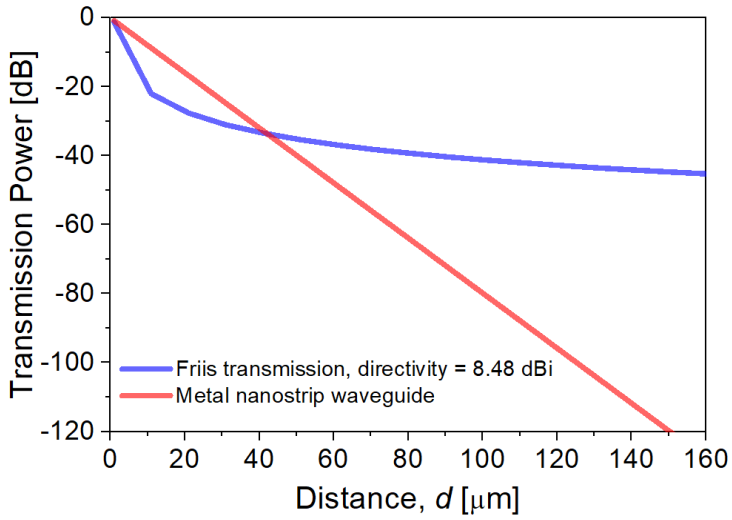

Figure 6. Comparison between wired (in red) and wireless link between MDMD nanostrip waveguide. For the wireless case are assumed directivity of 8.48 dBi (in blue).

3. CONCLUSION

We have reported numerical results about coupling characteristics of an NDRA coupled to an MDMD nanostrip waveguide. NDRAs can radiate broadside power; which is a very useful characteristic for a wide range of applications such as flexible and effective inter-chip wireless interconnections in the optical regime, including infrared and terahertz technologies. Furthermore, they exhibit interesting and impressive performances in terms of bandwidth and realized gain. The numerical results show that it can be used as an efficient approach to transmitting/couple optical energy

from/into plasmonic circuits. Furthermore, the NDRA can be a very promising device for applications based on integrating different planar lightwave circuit technologies.

REFERENCES

[1] Zia, R., Schuller, J. A., Chandran, A. and Brongersma, M. L., "Plasmonics: the next chip-scale technology," *Materials Today*, vol. 9, no. 7–8, pp. 20–27 (2006).

[2] Ozbay, E., "Plasmonics: Merging Photonics and Electronics at Nanoscale Dimensions," *Science*, vol. 311, no. 5758, pp. 189–193 (2006).

[3] Schuller, J. A., Barnard, E. S., Cai, W., Jun, Y. C., White, J. S. and Brongersma, M. L., "Plasmonics for extreme light concentration and manipulation," *Nature Materials*, vol. 9, no. 3, pp. 193–204 (2010).

[4] Seok, T. J. *et al.*, "Radiation Engineering of Optical Antennas for Maximum Field Enhancement," *Nano Lett.*, vol. 11, no. 7, pp. 2606–2610 (2011).

[5] Yu, N. *et al.*, "Flat Optics: Controlling Wavefronts With Optical Antenna Metasurfaces," *IEEE Journal of Selected Topics in Quantum Electronics*, vol. 19, no. 3, pp. 4700423–4700423 (2013).

[6] Cohen, M., Abulafia, Y., Lev, D., Lewis, A., Shavit, R. and Zalevsky, Z., "Wireless Communication with Nanoplasmonic Data Carriers: Macroscale Propagation of Nanophotonic Plasmon Polaritons Probed by Near-Field Nanoimaging," *Nano Lett.*, vol. 17, no. 9, pp. 5181–5186 (2017).

[7] Almeida, V. R., Panepucci, R. R. and Lipson, M., "Nanotaper for compact mode conversion," *Optics Letters*, vol. 28, no. 15, p. 1302 (2003).

[8] Bogaerts, W. *et al.*, "Nanophotonic waveguides in silicon-on-insulator fabricated with CMOS technology," *Journal of Lightwave Technology*, vol. 23, no. 1, pp. 401–412 (2005).

[9] Alù, A. and Engheta, N., "Wireless at the Nanoscale: Optical Interconnects using Matched Nanoantennas," *Physical Review Letters*, vol. 104, no. 21 (2010).

[10] Hosseini, A., Nejati, H. and Massoud, Y., "Design of a maximally flat optical low pass filter using plasmonic nanostrip waveguides," *Opt. Express*, vol. 15, no. 23, pp. 15280–15286 (2007).

[11] Mongia, R. K. and Bhartia, P., "Dielectric resonator antennas—a review and general design relations for resonant frequency and bandwidth," *International Journal of Microwave and Millimeter-Wave Computer-Aided Engineering*, vol. 4, no. 3, pp. 230–247 (1994).

[12] Malheiros-Silveira, G. N., Wiederhecker, G. S. and Hernández-Figueroa, H. E., "Dielectric resonator antenna for applications in nanophotonics," *Optics Express*, vol. 21, no. 1, p. 1234 (2013).

[13] Zou, L. *et al.*, "Dielectric resonator nanoantennas at visible frequencies," *Optics Express*, vol. 21, no. 1, p. 1344, (2013).

[14] Malheiros-Silveira, G. N., Gabrielli, L. H., Chang-Hasnain, C. J. and Hernandez-Figueroa, H. E., "Breakthroughs in Photonics 2013: Advances in Nanoantennas," *IEEE Photonics Journal*, vol. 6, no. 2, pp. 1–6 (2014).

[15] Zou, L. *et al.*, "Efficiency and Scalability of Dielectric Resonator Antennas at Optical Frequencies," *IEEE Photonics Journal*, vol. 6, no. 4, pp. 1–10 (2014).

[16] Malheiros-Silveira, G. N. and Hernandez-Figueroa, H. E., "Dielectric Resonator Nanoantenna Coupled to Metallic Coplanar Waveguide," *IEEE Photonics Journal*, vol. 7, no. 1, pp. 1–7 (2015).

[17] Malheiros-Silveira, G. N., Lu, F., Bhattacharya, I., Tran, T.-T. D., Sun, H., and Chang-Hasnain, C. J., "III-V Compound Semiconductor Nanopillars Monolithically Integrated to Silicon Photonics," *ACS Photonics*, vol. 4, no. 5, pp. 1021–1025 (2017).

[18] Malheiros-Silveira, G. N. and Hernández-Figueroa, H. E., "Wireless optical coupling evaluation in a dielectric resonator nanoantenna," *OSA Continuum*, vol. 1, no. 3, p. 805 (2018).

[19] Johnson, P. B. and Christy, R. W., "Optical Constants of the Noble Metals," *Phys. Rev. B*, vol. 6, no. 12, pp. 4370–4379 (1972).

[20] Balanis, C., *Antenna Theory: Analysis and Design, 3rd Edition*. Wiley-Interscience (2005).